Vacuum ultra-violet spectroscopic ellipsometry study of single- and multi-phase nitride protective films

2006 J. Phys.: Condens. Matter 18 S1691

(http://iopscience.iop.org/0953-8984/18/32/S01)

INSTITUTE OF PHYSICS PUBLISHING JOURNAL OF PHYSICS: CONDENSED MATTER

J. Phys.: Condens. Matter **18** (2006) S1691–S1701 doi:10.1088/0953-8984/18/32/S01

Vacuum ultra-violet spectroscopic ellipsometry study of single- and multi-phase nitride protective films

S M Aouadi[1], A Bohnhoff[1], T Amriou[2], M Williams[3], J N Hilfiker[4], N Singh[4] and J A Woollam[4]

[1] Department of Physics, Southern Illinois University, Carbondale, IL 62901-4401, USA
[2] Université d'Artois, Faculté Jean Perrin -SP18-, Rue Jean Souvraz, 62307 Lens Cedex, France
[3] Frederick Seitz Materials Research Laboratory, University of Illinois, Urbana, IL 61801, USA
[4] J A Woollam Co., Incorporated, 645 M Street, Suite 102, Lincoln, NE 68508, USA

Received 28 September 2005
Published 24 July 2006
Online at stacks.iop.org/JPhysCM/18/S1691

Abstract

This paper reports on a systematic investigation of the optical properties of $Ta_{1-x}Zr_xN$ single-phase and ZrN–Ag multi-phase films fabricated by unbalanced magnetron sputtering using vacuum ultraviolet spectroscopic ellipsometry (VUV-SE). VUV-SE is a newly developed technique that was used to evaluate the strength and energy of the interband electronic excitations/transitions in these films. The energy of the interband transition was found to be altered by any changes in the elemental composition for single-phase materials. For example, it was found to increase with the increase in the covalent character of the bond as more Zr atoms are substituted for by Ta atoms in the ZrN rock-salt structure. In contrast, the peak positions did not vary in the multi-phase structures because the constituent phases were immiscible and retained their electronic structure. However, the strength and width of the interband transition were found to change to reflect changes in phase composition and microstructure. The optical and electronic properties of these materials were simulated using density functional theory (DFT) within the generalized gradient approximation. The calculated refractive indices and density of states were in good agreement with the VUV-SE data.

1. Introduction

Transition metal nitrides have been used for over three decades as protective coatings for various applications including moulds, punches, cutting tools, machine parts for motors, diffusion barriers for integrated circuits, solar reflectors, and biomedical implants [1–8]. More recently, the addition of one or more elements was found to improve the properties of the more traditional binary nitride thin films. Depending on the thermodynamic properties of the compound to be formed and on process parameters, there are two alternative film designs that may be produced [9–15]: (1) the additional element(s) may substitute in the lattice of the

original material to form a single-phase material, or (2) there is phase segregation due to the immiscibility (or partial miscibility) of the additional element or compound and formation of a multi-phase material. A multitude of characterization techniques have been used to understand the contribution of the following factors that affect the overall mechanical properties of these materials: elemental and phase composition (single phase or multi-phase, and what phases are formed?), microstructure (grain size, film architecture), and bonding information. Some of the techniques that are routinely used to analyse these properties include x-ray diffraction (XRD), transmission electron microscopy (TEM), x-ray photoelectron spectroscopy (XPS), Rutherford backscattering (RBS), and ultra-violet photoelectron spectroscopy (UPS). Each of the listed techniques has its advantages and disadvantages and researchers usually necessitate two or more complementary techniques to evaluate most of the important physical and chemical properties that characterize any investigated sample.

Vacuum ultra-violet spectroscopic ellipsometry (VUV-SE) is a newly developed technique that extends the conventional range of SE to higher photon energies. In this region, the optical response for most materials is dominated by band-to-band transitions. Light is absorbed by the material to excite an electron from the occupied valence band to the unoccupied conduction band. Hence, the measured optical properties depend on the density of states in each band and on transition probabilities. Detailed discussions of material optical properties and their relationship to electronic structure can be found in many references [16, 17]. Since the bonding properties of a material may be correlated to its valence band electronic structure, VUV-SE might prove to be another useful technique that provides information about the bonding properties of a material. If VUV-SE is used in tandem with *ab initio* calculations based on density functional theory, this analytical tool may even be able to provide additional information about other physical and chemical characteristics of the material. In addition, bonding properties may be used to predict the intrinsic mechanical properties of a material. In general, bonding properties correlate well with the measured elastic modulus E since the latter depends mostly on the former [18]. However, the hardness of a material depends more on dislocation motion and the extrinsic contribution to the hardness, which results from the presence of defects in the film, becomes significant [18].

The objective of this work is to use VUV-SE as a technique to investigate single-phase and multi-phase ternary nitride-based protective coatings. The following materials were selected: $Ta_{1-x}Zr_xN$ [19] single phase and ZrN–Ag [19] two-phase nanocrystalline materials. Both materials are based on the addition of a single element (Ta or Ag) to ZrN. The mechanical properties of these two films were investigated by our group as a function of composition and deposition parameters in articles that were published earlier [19, 20]. The optical properties of these materials were evaluated using VUV-SE and the measured quantities were simulated using *ab initio* density functional theory calculations to elucidate the main contributions to the various measured quantities. Various experimental tools were subsequently utilized and include x-ray diffraction (XRD), Rutherford backscattering (RBS), and VUV-SE in order to determine their structure, chemical composition, and their interband electronic transitions, respectively.

2. Methodology

$Ta_{1-x}Zr_xN$ single-phase and ZrN–Ag multi-phase films with a thickness of 1.5 μm were deposited on Si(111) wafers by reactive unbalanced magnetron dc sputtering from individual metallic sources. The system, manufactured by AJA International, was described elsewhere [19, 20]. A system pressure of $\approx 1 \times 10^{-5}$ Pa was achieved prior to each film deposition. The Ar and N_2 pressures were set to 0.2 and 0.01 Pa, respectively, and the

Table 1. Deposition conditions and composition for TaZrN and ZrN–Ag film samples.

Sample	Power to Ta or Ag target (W)	Ag (%)	Ta (%)	Zr (%)	N (%)
TA1	0	—	0	50 ± 2	50 ± 2
TA2	13	—	10 ± 2	36 ± 2	53 ± 4
TA3	20	—	14 ± 2	34 ± 2	60 ± 4
TA4	34	—	22 ± 2	27 ± 2	59 ± 4
AG1	0	0	—	50 ± 2	50 ± 2
AG2	2	6 ± 2	—	46 ± 2	48 ± 4
AG3	3	9 ± 2	—	45 ± 2	46 ± 4
AG4	4	13 ± 2	—	43 ± 2	44 ± 4
AG5	5	18 ± 2	—	41 ± 2	41 ± 4

films were produced using a bias voltage of −70 V. The substrate was not heated during the deposition of ZrN–Ag and was heated to 440 °C during the growth of $Ta_{1-x}Zr_xN$. The power to the Zr target was kept at 70 W. The power to the additional target (for Ta or Ag) was varied as shown in table 1. The crystallographic structure of the films was analysed using 1.54 Å wavelength Cu Kα radiation with a Rigaku Geigerflex D-MAX x-ray diffractometer and a graphite diffracted beam monochromator. The chemical composition was determined using Rutherford backscattering (RBS). The RBS probe consisted of 2 MeV He^+ ions incident at an angle of 22.5° relative to the sample surface normal with the detector set at a 150° scattering angle. The VUV-VASE™ variable angle spectroscopic ellipsometer for the vacuum ultraviolet was used to measure the optical response of our films in the spectral ranging from 130 to 1700 nm. Two angles of incidence were used during measurement: 60° and 75°. The entire optical path is enclosed inside a dry nitrogen purge to eliminate absorption from ambient water vapour and oxygen. A convenient sample load cell allows access to the stage to load samples up to 300 mm in diameter. The VUV-VASE uses a rotating analyser ellipsometer (RAE) configuration with the addition of an AutoRetarder™. The AutoRetarder adds a computer controlled MgF2 Berek waveplate into the optical path of the rotating analyser ellipsometer configuration. The amount of retardation can be automatically adjusted to provide higher accuracy measurements [21].

3. Computational method

The ground state energies, optical constants, and electronic structure of ZrN, $Ta_{1-x}Zr_xN$, and Ag were calculated within the density functional theory (DFT) formalism using CASTEP (Cambridge Sequential Total Energy Package) software [22–25]. CASTEP uses a total energy plane-wave pseudo-potential method. In the mathematical model of the material, CASTEP replaces ionic potentials with effective potentials acting only on the valence electrons in the system. The electronic wavefunctions were expanded with a plane-wave basis set-up to a plane-wave cut-off energy sufficient for convergence, which varies depending on the convergence of each pseudopotential. The electronic energies were mapped to a set of special k-points in the reduced Brillouin zone and the number of k-points was determined by the spacing in the reciprocal space. The exchange–correlation functional used in this study was the gradient corrected local density approximation of Perdew and Wang, or GGA-PW91 [26]. In order to achieve a high level of convergence of the total energy, a plane-wave cut-off of 360 eV was selected. The total self-consistent field (SCF) energy change was 5×10^{-6} eV/atom and the energy between optimization steps was 5×10^{-5} eV/atom. An eight-atom cubic unit cell

model with rock-salt structure was used to calculate the optical constants and density of states for ZrN and $Ta_{1-x}Zr_xN$. In order to study the effect of alloying on the various properties of the films, one or more Zr atoms were replaced by Ta atoms in the ZrN lattice. Similarly, an FCC structure was utilized to calculate the optical constants and the density of states for crystalline Ag.

4. Results and discussion

4.1. TaZrN system

XRD measurements indicated that these samples formed a single-phase solid solution typical of a rock-salt structure. A general shift in the 2θ-positions towards higher d-values was observed with increasing tantalum content in the films. In addition, the average grain sizes were calculated from the widths of the XRD peaks and were found to be independent of the amount of Ta in the sample (about 28 nm). The elemental composition deduced from RBS measurements is reported in table 1. A more detailed analysis of the structural and chemical properties of these materials may be found in a recently published article [19].

Figure 1 shows the measured refractive index and absorption coefficient as a function of wavelength. This figure indicated that the addition of tantalum had an effect on the intraband (larger wavelengths) and interband electronic contributions (peak around 245 nm) to the optical response of the films. Measuring the optical constants of a material gives a powerful insight into their electronic band structure since it can show the various allowed carrier excitations (electron transitions). As a result, the measured optical data in figure 1 were modelled as a superposition of a Drude term and two Lorentz oscillator terms. The Drude term corresponds to contributions from the free-electron gas (intraband transitions or transitions between two states in the same band) to the dielectric function whereas the Lorentz oscillator terms describe contributions from bound electrons (interband transitions between two states in different bands) [27, 28]. The Lorentz terms are more relevant for the understanding of the electronic structure of these films: interband transitions between bands are specific to the constituent phases of the investigated materials. In contrast, the contribution from the free electron gas is more prone to defects and is affected substantially by scattering from imperfections such as grain boundaries, vacancies, interstitials, etc.

Figure 2 shows the variation of the centre energy of the two Lorentz oscillators that correspond to transitions from the e_g and t_{2g} bands with Ta content [29]. These results indicate that there is a shift in the peak position, represented by E, of the Lorentz oscillators to higher energies (lower wavelengths). The peak position of the interband transitions depends on the stoichiometry of the films and may be used as a tool to predict the chemical composition of the films.

Figure 3 shows the theoretical and experimental refractive index and absorption coefficient for ZrN. The peak positions and widths for n and k were reproduced by the simulation. For example, the peak position for n was 245 and 235 nm for the measured and the calculated spectra, respectively. This insignificant difference could be due to various factors including computational errors and the non-stoichiometry of the films. Our samples are also slightly over-stoichiometric, and this would lead to a slight shift in the peak position to higher energies, as predicted by our simulations (not shown here), due to the less metallic character nature of the bonds. The peak shifts observed experimentally with increasing Ta content in the films were accurately predicted by the simulation when Zr atoms are substituted for by Ta atoms.

To explain the optical properties discussed above, the theoretical partial p- and d-state densities for $Ta_{1-x}Zr_xN$ were calculated for $x = 0.00, 0.25, 0.50$, and 1.0 (figure 4). The

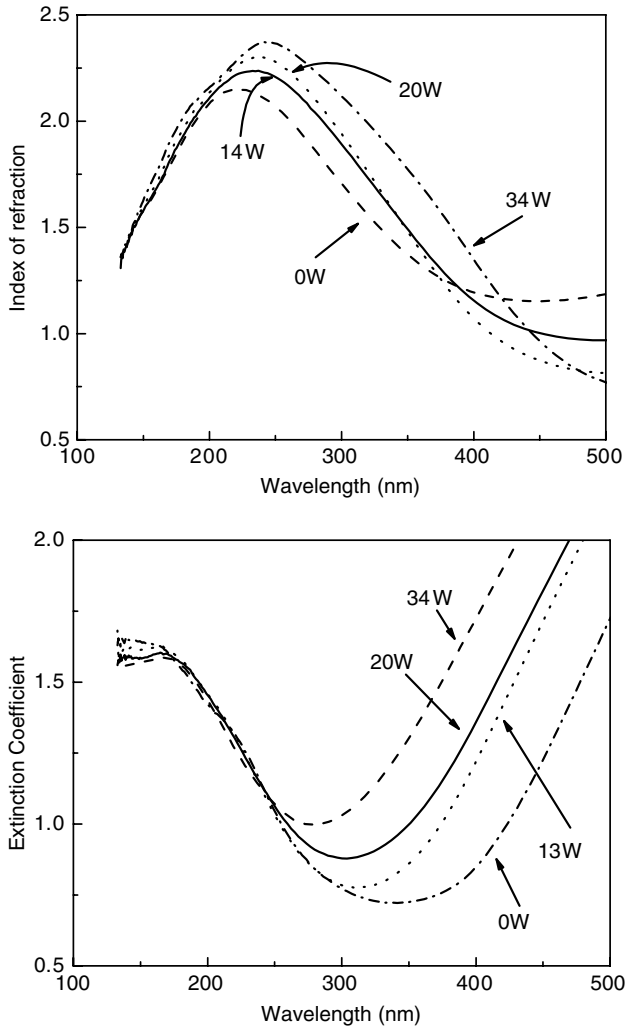

Figure 1. Experimental refractive index and absorption coefficient for $Ta_{1-x}Zr_xN$ films.

DOS for ZrN consists of a broad peak between −8 and −3 eV, a feature that is loosely referred to as the 2p band, which originates from the non-metal 2p orbitals hybridizing with the metal d orbitals [29]. This feature actually corresponds to a double-peaked structure with the d contribution in the 2p band of both e_g and t_{2g} symmetry, with the e_g part dominating. The e_g and t_{2g} peaks are centred at 5.0 and 6.5 eV for ZrN ($x = 0.0$). A shift to higher energies by about 1.0 eV results from the variation of x from 0.0 to 0.5, which corresponds to a film composition of $Ta_{0.5}Zr_{0.5}N$. These observations are in agreement with the shift of 1.0 eV shown in figure 2 that corresponds to transitions from the e_g and t_{2g} bands. The non-metal 2p orbital hybridization with the metal d orbitals is strongest for the TaN system. The intrinsic hardness and elastic modulus are therefore expected to be higher for TaN than for ZrN.

4.2. ZrN–Ag system

The structure of ZrN and ZrN–Ag films was determined by XRD [20]. The films were found to exhibit strong ZrN(200) and (111) preferred orientations. The width of the two peaks

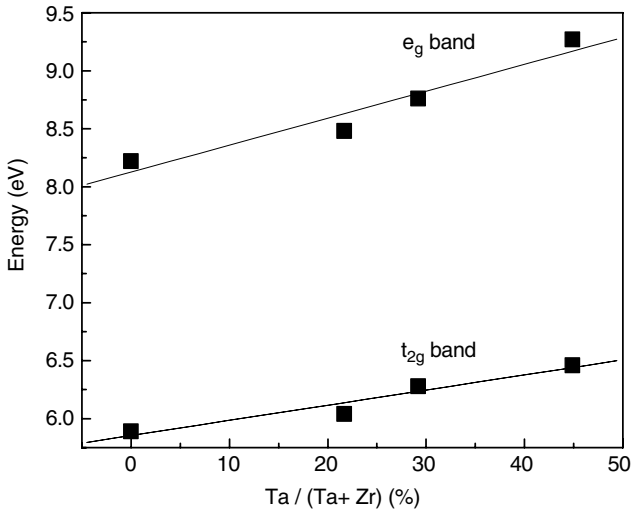

Figure 2. Energy of the interband transitions for $Ta_{1-x}Zr_xN$ films determined from simulating the VUV-SE data with a Drude–Lorentz oscillator model.

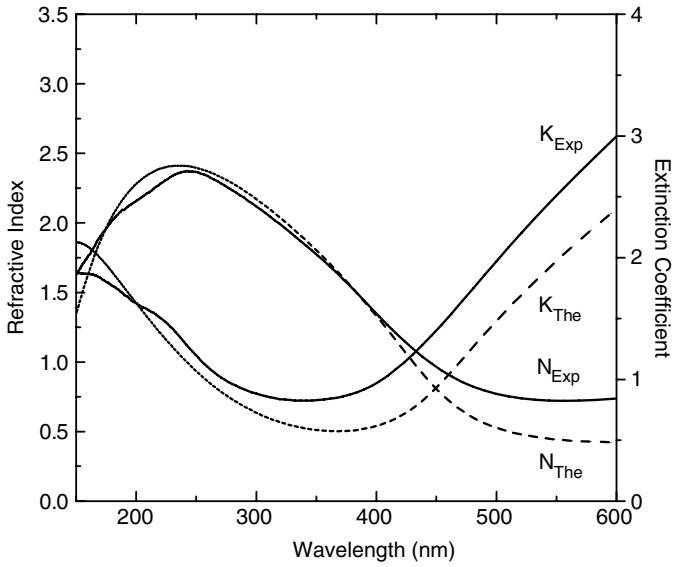

Figure 3. Overlay of experimental and theoretical refractive indices for ZrN films.

increased significantly with the addition of silver, which indicated that the grain size became very small. The matrix, i.e. silver, was primarily XRD amorphous. The average grain sizes for ZrN nanocrystals were calculated from the widths of the XRD peaks using the Scherrer formula and were found to decrease from 25 to 8 nm. The Ag content was determined by RBS and is listed in table 1. XRD measurements in tandem with TEM measurements (not shown here) suggest that these films consisted of ZrN nanocrystals embedded in a silver matrix [20].

Figure 5 shows the refractive index and absorption coefficient for ZrN–Ag films as a function of wavelength. The data were simulated using a Drude–Lorentz model and the

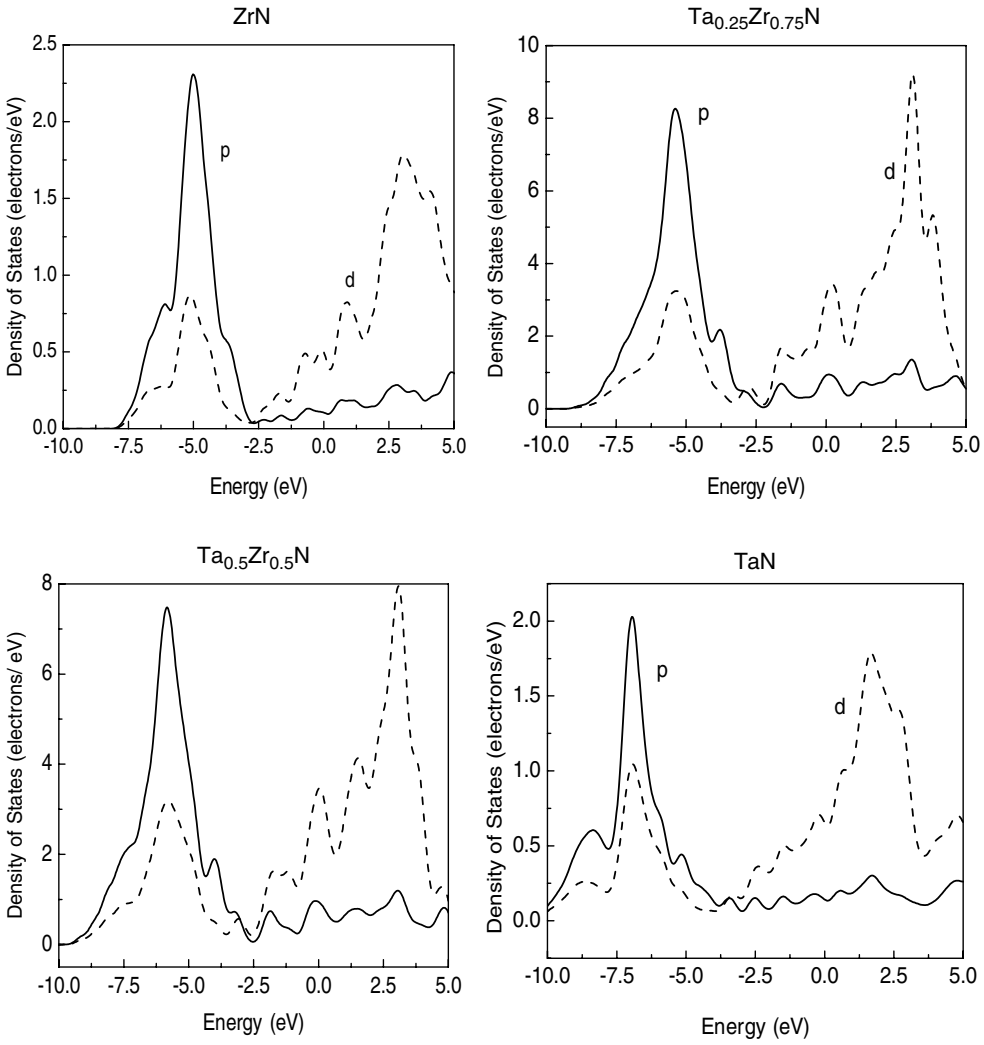

Figure 4. Calculated DOS for $Ta_{1-x}Zr_xN$.

results of the simulation indicate major differences between the optical response for ZrN–Ag and $Ta_{1-x}Zr_xN$ films. First, the simulation for Ag–ZrN required an additional Lorentz oscillator, centred at 4.4 eV, which suggests the formation of a second phase. Second, the peaks that correspond to transitions from the e_g and t_{2g} bands to the conduction band remained fixed, which suggested the immiscibility of the two phases that constitute the nanocomposite structure. The two phases were previously shown to be immiscible using XRD and XPS [20]. Finally, the strength of the three peaks, shown in figure 6, varied with changes in the phase composition and reflects a decrease in ZrN content and an increase in Ag content. In addition, the three peaks became broader due to the grain refinement that resulted from the formation of a nanocomposite structure [30].

To explain the optical properties of the Ag phase in the nanocomposite structure, the theoretical density of states for crystalline Ag was calculated and is shown in figure 7. The DOS for the ZrN phase has already been shown in the previous sub-section (figure 4). The

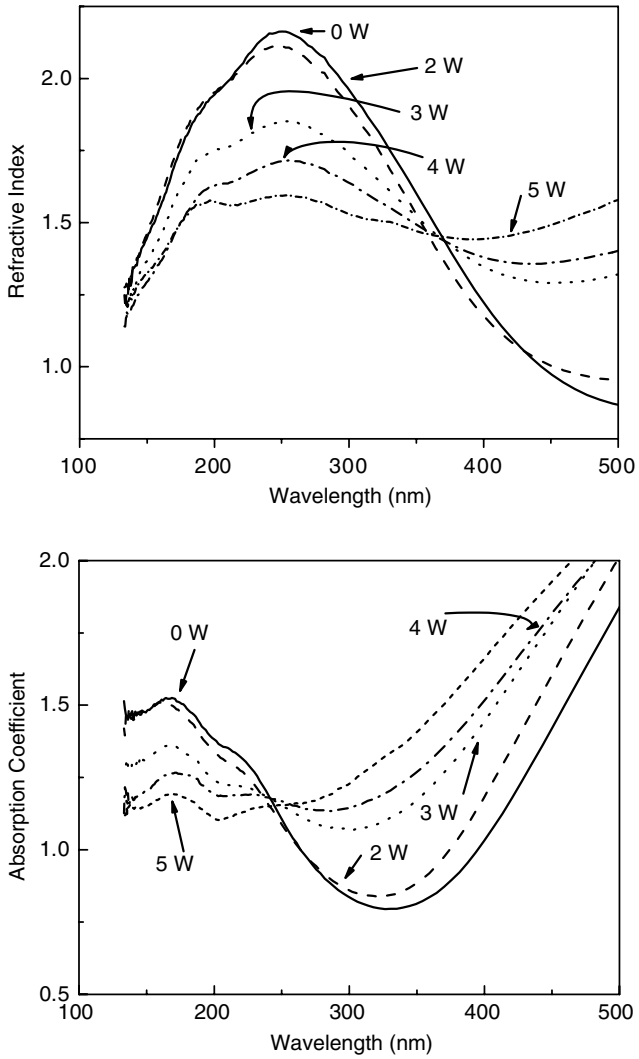

Figure 5. Experimental refractive index and absorption coefficient for the ZrN–Ag films.

DOS for crystalline Ag consists of a broad peak between −5 and −2 eV, which corresponds to the 4d orbitals of Ag. Only one Lorentz oscillator was required to simulate Ag because the features observed for crystalline Ag are smeared out as a result of the amorphous nature of the phase.

4.3. Discussion

The results presented in this paper show the potential of combining VUV-SE and DFT calculations to provide important information about novel protective films, namely single-phase and multi-phase nanostructures. This is due to the fact that VUV-SE probes the electronic structure of these films, which depends on elemental/phase composition and the presence of defects in the films. In the case of ternary compounds, for example, if the energy of the interband transition shifts with the addition of the third element, then this element is soluble in

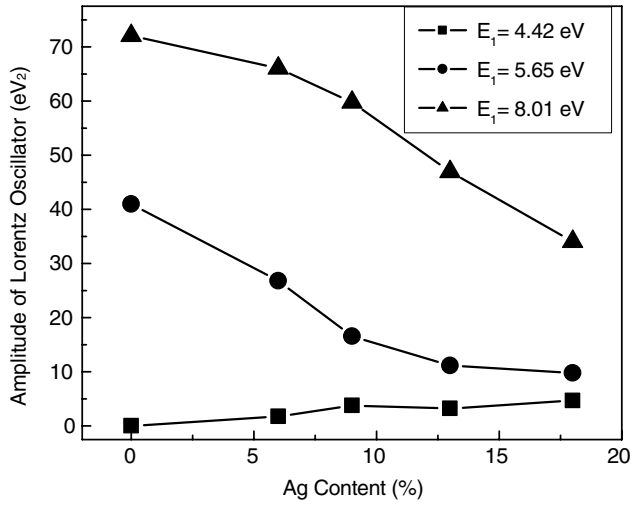

Figure 6. Strength of the Lorentz oscillators as a function of Ag content.

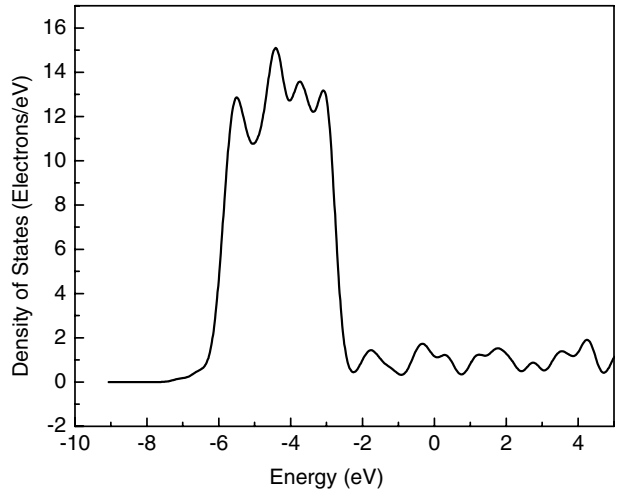

Figure 7. Calculated DOS for Ag.

the initial binary phase. Also, there is total solubility if there are no new interband transitions that contribute to the optical response of the films; otherwise, the solubility may be limited. The phase information provided by VUV-SE is, therefore, similar to the data inferred from XRD. In the case of $Ta_{1-x}Zr_xN$, there was total solubility since no new Lorentz oscillator was required to model the films in the range investigated in this work. In the case of ZrN–Ag, however, VUV-SE indicated the formation of a second phase, as revealed by the additional Lorentz oscillator at 4.4 eV. Moreover, the energy of the Lorentz oscillators that correspond to ZrN or Ag did not vary, which suggested the immiscibility of these phases.

VUV-SE may provide bonding information as well. For single-phase ternary materials, for example, the energy shift in the Lorentz oscillator provides information about changes in the bonding structure of the films. Shifts to higher energies, as was the case for $Ta_{1-x}Zr_xN$, indicate a more covalent bond since the interband transitions provide information about the

valence band. Shifts in the electronic structure have been used by many workers to study the nature of the bonds using UPS (shifts in the valence band) or XPS (shifts in deeper bands). So, VUV-SE is similar to UPS or XPS in that it probes the electronic structure of these materials. But unlike UPS and XPS, VUV-SE is not a destructive technique since it does not require that the surface impurities and oxide layer be sputter-etched prior to making measurements. Finally, VUV-SE can provide quantitative data as well. In single-phase ternary materials, for example, the peak position of the Lorentz oscillators may be correlated to the elemental composition since it varies linearly with the content of the additional element. *Ab initio* calculations may be used in tandem with VUV-SE to provide such information more readily. In addition, in the case of nanocomposite structures, a correlation between the areas under the curves for the various phases may be made to explain changes in phase compositions.

5. Conclusions

In this paper, thin films of $Ta_{1-x}Zr_xN$ and Ag–ZrN were deposited using reactive unbalanced magnetron sputtering from dual sources. The $Ta_{1-x}Zr_xN$ and Ag–ZrN films formed a solid solution and a nanocomposite structure, respectively. Rutherford backscattering was used to determine the chemical composition of the films. Vacuum ultraviolet spectroscopic ellipsometry was used to evaluate the strength and energy of their interband electronic excitations/transitions and, hence, indirectly probe the valence band electronic structure. The electronic structure (density of states) and the optical response (dielectric function) of the films were simulated using *ab initio* density functional theory. An excellent agreement between the theoretical and experimental data was observed. For single-phase ternary nitrides, the valence band shifted by 1.0 eV for $x = 0$–0.5, indicating that the bonds are more covalent. For nanocomposite structures, the optical response was a superposition of the optical response of the constituent phases and no changes in the energy of the Lorentz oscillators were observed, indicating the total immiscibility of the two phases. This study has provided an understanding of the various contributions to the optical properties of single and multi-phase nanocrystalline protective films and could enable the prediction of the optical properties of novel nitride materials as well. Optical properties in the VUV are dominated by high-photon energy electronic transitions from the valence to conduction band and provide important information about the electronic structure of these materials, which can, in turn, be correlated to bond strength, elemental composition, vacancies, etc. In addition, the bonding properties of these materials may be associated with their 'intrinsic' mechanical properties.

Acknowledgments

The authors would like to thank Professor I Petrov for RBS measurements carried out in the Center for Microanalysis of Materials, University of Illinois, which is partially supported by the US Department of Energy under grant DEFG02-91-ER45439. This research was supported by an award from the Research Corporation, by the Materials Technology Center of Southern Illinois University and by the J A Woollam Co.

References

[1] Sproul W D 1986 *Thin Solid Films* **107** 141
[2] Mitterer C, Ubleis A and Ebner R 1991 *Mater. Sci. Eng.* A **140** 670
[3] Sproul W D, Graham M F, Wong M S and Rudnick P J 1993 *Surf. Coat. Technol.* **61** 139
[4] Andrievski R A, Anisimova I A, Anisimov V P, Makarov V P and Popova V P 1995 *Thin Solid Films* **261** 83

[5] Ribbing C G and Roos A 1997 *Proc. Int. Soc. Opt. Eng.* **3133** 148
[6] Nose M, Nagae T, Yokota M, Saji S, Zhou M and Nakada M 1999 *Surf. Coat. Technol.* **116** 296
[7] Wiedemann R, Weihnacht V and Oettel H 1999 *Surf. Coat. Technol.* **116–119** 302
[8] Aouadi S M, Shreeman P K and Williams M 2004 *J. Appl. Phys.* **96** 3949
[9] Hasegawa H and Suzuki T 2004 *Surf. Coat. Technol.* **188/189** 234
[10] Vepřek S, Vepřek-Heijman M J G, Karvankova P and Prochazka J 2005 *Thin Solid Films* **476** 1
[11] Hauert R and Patscheider J 2000 *Adv. Eng. Mater.* **2** 247
[12] Musil J, Vlcek J, Regent F, Kunc F and Zeman H 2002 *Key Eng. Mater.* **230–232** 613
[13] Voevodin A A and Zabinski J S 2005 *Comput. Sci. Technol.* **65** 741
[14] Zhang S, Sun D, Fu Y and Du H 2003 *Surf. Coat. Technol.* **167** 113
[15] Kraznowski J E 2004 *Surf. Coat. Technol.* **188/189** 376
[16] Adachi S 1999 *Optical Properties of Crystalline and Amorphous Semiconductors: Materials and Fundamental Principles* (Boston, MA: Kluwer–Academic)
[17] Amirtharaj P M and Seiler D G 1995 *Handbook of Optics* 2nd edn, vol 2 *Devices, Measurements, and Properties* ed M Bass (New York: McGraw-Hill)
[18] Shin C-S, Gall D, Hellgren N, Patscheider J, Petrov I and Greene J E 2003 *J. Appl. Phys.* **93** 6025
[19] Aouadi S M, Filip P and Debessai M 2004 *Surf. Coat. Technol.* **187** 177
[20] Aouadi S M, Debessai M and Filip P 2004 *J. Vac. Sci. Technol.* B **22** 1134
[21] Johs B, Woollam J A, Herzinger C M, Hilfiker J, Synowicki R and Bungay C L 1999 *Proc. Int. Soc. Opt. Eng.* **CR72** 29
[22] Dreizler R M and Gross E K U 1990 *Density Functional Theory* (Berlin: Springer)
[23] Milman V, Winkler V, White J A, Pickard C J, Payne M C, Akhmatskaya E V and Nobes R H 2000 *Int. Quantum Chem.* **77** 895
[24] Payne M C, Teter M P, Allan D C, Arias T A and Joannopoulos J D 1992 *Rev. Mod. Phys.* **64** 1045
[25] Segall M D, Lindan P J D, Probert M J, Pickard C J, Hasnip P J, Clark S J and Payne M C 2002 *J. Phys.: Condens. Matter* **14** 2717
[26] Wang Y and Perdew J P 1991 *Phys. Rev.* B **43** 8911
[27] Wootten F 1972 *Optical Properties of Solids* (New York: Academic)
[28] Patsalas P and Logothetidis S 2003 *J. Appl. Phys.* **93** 989
[29] Delin A, Eriksson O, Ahuja R, Johansson B, Brooks M S S, Auluck S and Wills J M 1996 *Phys. Rev.* B **54** 1673
[30] Petrov I, Barna P B, Hultman L and Greene J E 2003 *J. Vac. Sci. Technol.* A **21** S117